

# A Low-Voltage Low-Power Current-Mode High-Pass Leapfrog Filter

WOUTER A. SERDIJN

*Delft University of Technology, Department of Electrical Engineering, Electronics Research Laboratory, Mekelweg 4, 2628 CD Delft, The Netherlands*

**Abstract.** A low-power bipolar continuous-time low-frequency high-pass second-order Butterworth filter is presented that works in the current domain and operates from a single 1.3-V battery. The filter contains two adjustable integrators. These integrators are realized by means of a capacitance and an adjustable transconductance amplifier with an indirect output. The complete filter, including all capacitances needed, can be integrated in an ordinary full-custom IC process. A semicustom realization is shown. The filter demonstrates operation down to 1 V with less than 16  $\mu\text{W}$  power consumption and a dynamic range of 50 dB. Its cutoff frequency can be exponentially tuned with a control current over a range from 100 Hz to 1 kHz.

Received November 11, 1991; Revised April 8, 1992.

## 1. Introduction

As the size and power consumption of electronic circuits is becoming more and more important, the demand for circuits that use a single battery and consume little current is increasing. Examples are hand-carried radiotelephones, pagers, and hearing instruments (see, e.g., [1–4]). To improve the speech intelligibility in these systems, especially of consonants, often a high-pass filter is used [5–7]. Apart from operating at “low-voltage level” (i.e., 1–1.3 V) and consuming as little current as possible to ensure long battery life, the filter bandwidth must be programmable to ensure a wide application area. Moreover, external components need to be avoided as much as possible.

This paper deals with the design and measurement of a fully integrated second-order high-pass Butterworth filter that meets all former specifications and whose cutoff frequency can be varied from 100 Hz to 1 kHz. In Sections 2–4, successively, the filter design is followed from a suitable filter architecture, via the elementary building blocks, up to their signal path. Together with a proper biasing circuit these blocks form the complete filter, as described in Section 5. Section 6 deals with a semicustom realization of which, in Section 7, measurement results are given.

## 2. A First Approach

To reduce the complexity and power consumption of the circuit to a minimum, we have chosen for an analog,

continuous-time filter. A passive, lossless  $LC$  filter would offer the best solution, but as the adjustability of such filters is weak and inductors cannot be integrated, we will have to simulate the network equations of the filter by means of “analog computer techniques.” This results in a “leapfrog filter” [8, 9]. The inductances and capacitances in a passive  $LC$  filter can be seen as elements that perform mathematical operations, like integrating and differentiating. These operations on the voltages or currents in the circuit are now performed by active circuits. Because a one-to-one relationship exists between the time constant of each active circuit and the value of a reactive element in the  $LC$  filter, also the sensitivity of the transfer function of a leapfrog filter to its component values is low.

Figure 1 shows a possible implementation of a second-order high-pass Butterworth leapfrog filter. The filter consists of integrators (because of their frequency stability [10]) and current mirrors with multiple outputs and has a current as the information carrying quantity, to reduce the influence of parasitic admittances [11]. The right current mirror provides three output signals: one equals the (inverted) input signal, the other two equal half the input signal. The input-output relation  $H(f)$  is given by

$$H(f) = \frac{i_o}{i_i} = \frac{1}{f^2 + j\sqrt{2}f_c/f + f_c^2/f^2} \quad (1)$$

in which  $f_c$  equals the cutoff frequency of the filter. Note that for every  $f_c$  the filter response is maximally flat (i.e., a Butterworth characteristic).

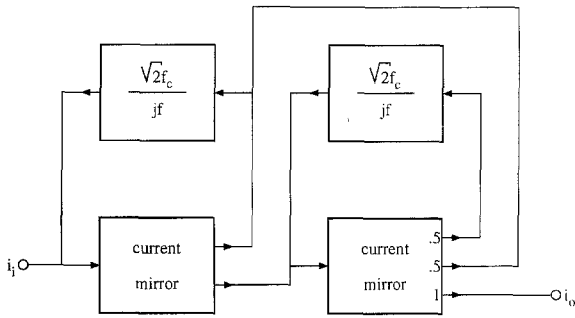


Fig. 1. Implementation of a second-order high-pass Butterworth leapfrog filter operating in the current domain.

### 3. The Integrator Blocks

As the integrator is to be realized in an integrated circuit, the integrating element must be a capacitor. The input signal of this capacitor is a current, whereas the output signal is a voltage. Therefore, an integrator operating in the current domain will always consist of a capacitor followed by a transconductance amplifier. This configuration is shown in figure 2. The amplifier has an indirect output [12]. Hence the possible output swing is maximized. Moreover, the filter is easily tuned by changing the scaling factor  $n$ , as will be shown subsequently.

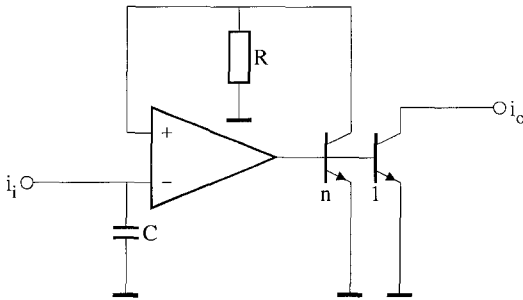


Fig. 2. Implementation of the integrator: a capacitance-transconductance amplifier with an indirect output.  $n$  is a scaling factor.

### 4. The Capacitance-Transconductance Amplifier

A possible implementation of the capacitance-transconductance amplifier is shown in figure 3. The capacitance  $C$  transforms the input current  $i_i$  into a voltage  $v_i = i_i / j2\pi fC$ , that in turn is transformed by  $Q_1$ ,  $Q_2$ , and resistance  $R$  into a current  $i_o' = v_i / R = i_i / j2\pi fRC$ .  $Q_3$  provides the indirect output. When the current through  $Q_3$  is  $n$  times as small as the current

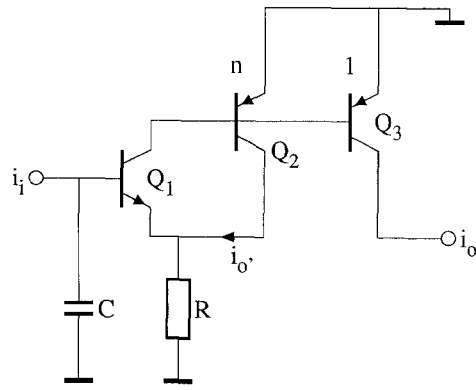


Fig. 3. Circuit diagram of the capacitance-transconductance amplifier.

through  $Q_2$  (and when the Early effect is negligible) we find

$$i_o = \frac{i_i}{j2\pi f n R C} \quad (2)$$

Combining (1) and (2) we find that the transfer functions  $H_t$  must satisfy

$$H_t = \frac{1}{nR} = 2\pi\sqrt{2} f_c C \quad (3)$$

#### 4.1. Noise Optimization

To calculate the amount of noise the capacitance-transconductance amplifier contributes to its output current, we shift the dominating noise sources (i.e., the noise sources of  $Q_1$ ) to the output, integrate the noise-power density spectrum over the total audio frequency range, and we find an expression for the equivalent noise current at the output,  $i_{n,eq}$  (see also appendix):

$$i_{n,eq} = \sqrt{\frac{2kT(f_2 - f_1)}{n^2} \left( \frac{1}{R^2 g_m} + \frac{g_m}{4\pi^2 B_F f_1 f_2 R^2 C^2} \right)} \quad (4)$$

with  $f_1$  the lowest frequency,  $f_2$  the highest frequency,  $g_m$  the transconductance factor of  $Q_1$ , and  $B_F$  the (low-frequency) current gain factor of  $Q_1$ . Obviously,  $C$  has to be chosen as large as possible. In addition, this expression can be minimized by varying  $g_m$ . Because  $g_m$  is proportional to the collector current of  $Q_1$ ,  $I_{C,Q_1}$ , it is possible to minimize (4) by varying  $I_C$ . For this optimum value,  $I_{C,Q_1,opt}$ , we find

$$I_{C,Q_1,opt} = \frac{kT}{q\sqrt{R^2/B_F + 1/4\pi^2 B_F C^2 f_1 f_2}} \quad (5)$$

#### 4.2. Collector Currents of $Q_2$ and $Q_3$

The maximum output signal,  $i_{t,\max}$  of the transconductance amplifier can be determined from its maximum input signal,  $v_{t,\max}$ , which is, in fact, the maximum voltage across the capacitor. Therefore

$$v_{t,\max} = \frac{i_{t,\max}}{H_{t,\min}} \quad (6)$$

With (3) it follows that

$$i_{t,\max} = v_{t,\max} H_{t,\min} = v_{t,\max} 2\pi\sqrt{2} f_{c,\min} C \quad (7)$$

As  $i_{t,\max}$  is delivered by  $Q_3$ , the collector current of  $Q_3$ ,  $I_{C,Q_3}$  is chosen best at least to be  $i_{t,\max}$ . A practical value of 1.2 times  $i_{t,\max}$  will do. As the filter has to operate at voltages down to 1 V,  $v_{t,\max}$  has been chosen equal to 100 mV.

The tuning of the filter is done by varying the factor  $n$ , which equals the collector current of  $Q_2$ ,  $I_{C,Q_2}$  divided by the collector current of  $Q_3$ ,  $I_{C,Q_3}$ . With (3) it follows that

$$I_{C,Q_2} = n I_{C,Q_3} = \frac{1}{2\pi\sqrt{2} f_c RC} I_{C,Q_3} \quad (8)$$

#### 4.3. Efficiency of the Capacitance-Transconductance Amplifier

Only a proper choice of the resistance  $R$  remains. Therefore we look at the efficiency  $\eta$  of the integrator, defined as follows:

$$\eta = \frac{\text{maximum signal current at the output}}{\text{total current of the integrator}} \quad (9)$$

or

$$\eta = \frac{I_{C,Q_3}}{I_{C,Q_1} + (n + 1)I_{C,Q_3}} \quad (10)$$

In order to obtain a good efficiency we see that it is convenient to choose  $n$  smaller than one for all cutoff frequencies possible. With (3) it follows that

$$n = \frac{1}{2\pi\sqrt{2} f_c RC} > 1 \quad \forall f_c \quad (11)$$

and thus

$$R > \frac{1}{2\pi\sqrt{2} f_{c,\min} C} \quad (12)$$

In practice this easily leads to values of  $R$  that cannot be integrated. For example, if  $f_{c,\min} = 100$  Hz and  $C = 400$  pF this results in  $R > 2.8$  M $\Omega$ . In most standard bipolar IC processes the value of a diffused resistor is limited to several hundred kilohms. So in that case the value of  $R$  can best be chosen maximally.

### 5. The Complete Filter

When we combine two capacitance-transconductance amplifiers with two current mirrors having multiple outputs according to the block diagram of figure 1, we have completed the signal path of the complete filter (figure 4). The (adjustable) scale factor  $n$ , which determines the cutoff frequency of the filter, is obtained by means of an adjustable voltage source  $V_f$ :

$$n = e^{V_f/V_T} \quad (13)$$

With (3) it follows that

$$f_c = \frac{1}{2\pi\sqrt{2} nRC} = \frac{e^{-V_f/V_T}}{2\pi\sqrt{2} RC} \quad (14)$$

This exponential relation between  $V_f$  and the cutoff frequency enables us to adjust the cutoff frequency over a wide range. If  $V_f$  is made proportional to the absolute temperature (PTAT) the cutoff frequency is independent of the temperature.

The complete filter, including its biasing scheme, is depicted in figure 5. GM-compensated mirrors [13] with multiple outputs provide the bias currents of every stage. When the voltage across  $R_1$  and  $R_2$  equals the thermal voltage  $V_T (= kT/q)$ , the output of the mirror is insensitive to its input ( $I_1$  and  $I_2$ ). At this point  $I_1$  and  $I_2$  equal  $e$  times the output currents  $I_{C,Q_1,\text{opt}}$  and  $I_{C,Q_3}$ , respectively. With (5) and (7) it follows that

$$I_1 = e I_{C,Q_1,\text{opt}} = e \frac{kT}{q\sqrt{R^2/B_F + 1/4\pi^2 B_F C^2 f_1 f_2}} \quad (15)$$

$$I_2 = e I_{C,Q_3} = e 1.2 v_{t,\max} 2\pi\sqrt{2} f_{c,\min} C \quad (16)$$

$$R_1 = \frac{kT}{qI_1} \quad (17)$$

$$R_2 = \frac{kT}{qI_2} \quad (18)$$

The currents  $I_1$  and  $I_2$  come from an external circuit which controls whether the filter is on or off (standby position). Transistors  $Q_A$  through  $Q_E$  provide the collector currents of  $Q_{2A}$  and  $Q_{2B}$ . The voltage source  $V_f$

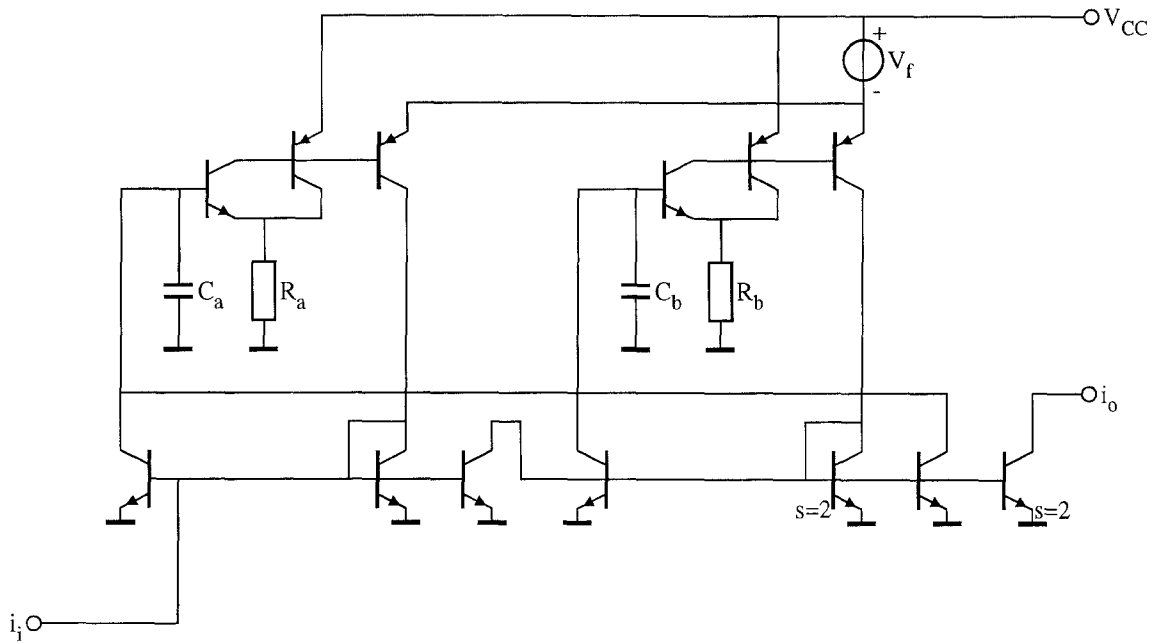


Fig. 4. Signal path of the complete filter,  $s = 1$  means a doubled emitter area ration.

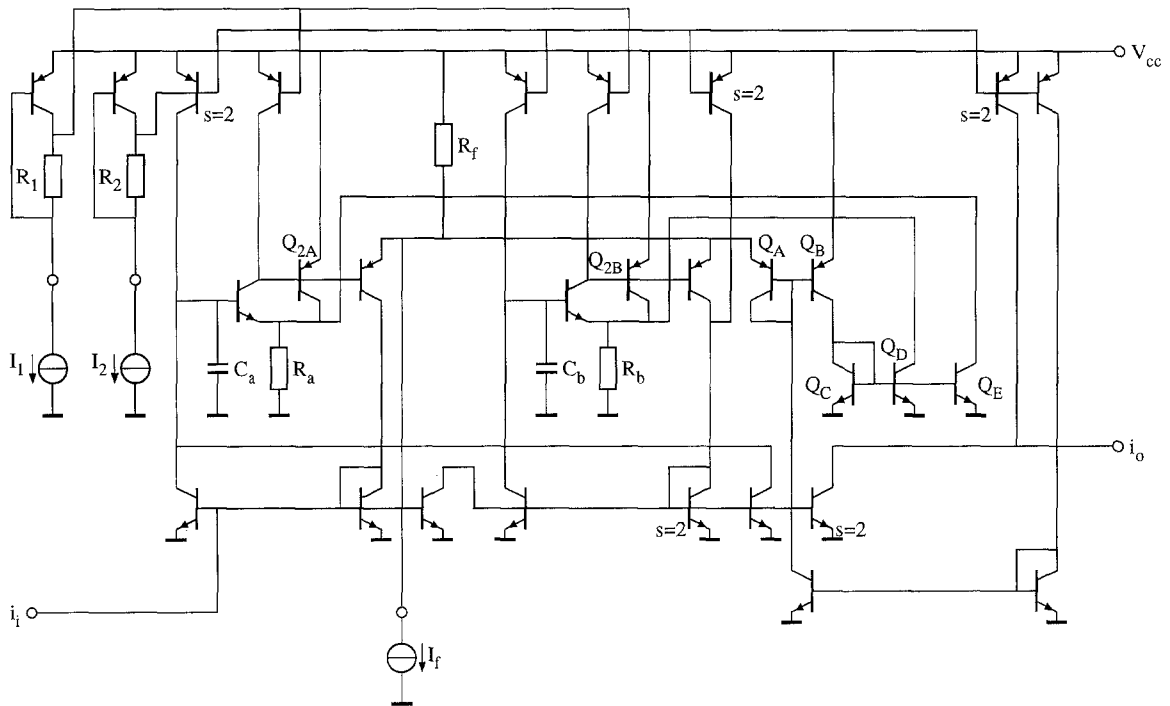


Fig. 5. The filter including its biasing scheme.  $s = 2$  means a doubled emitter area ratio.

is realized by a single resistor  $R_f$  through which flows a current  $I_f$  that is derived from an external circuit (e.g., a potentiometer or a programmable current source):

$$I_f = \frac{V_f}{R_f} = - \frac{V_T}{R_f} \ln(2\pi\sqrt{2} f_c RC) \quad (19)$$

Besides this current  $I_f$ , two emitter currents also contribute to the voltage over  $R_f$ . Because they contain an

ac component as well, this results in distortion of the output signal at higher input signal levels. This distortion can be made sufficiently small by choosing  $R_f$  smaller and  $I_f$  larger. Unfortunately, this degrades the efficiency of the filter. An acceptable compromise is therefore to be found with the aid of computer simulations. It turns out that this is possible. In critical situations the distortion can be reduced by means of a buffered voltage source [14].

## 6. Semicustom Realization

The active circuitry of figure 5 was integrated in a semicustom chip in the LA251 process [15]. Figure 6 shows a microphotograph of the chip. The two integrating capacitors  $C_A$  and  $C_B$  were chosen 400 pF. The two (diffused) resistors  $R_A$  and  $R_B$  were chosen to be 200 k $\Omega$ . These values can be integrated easily in an ordinary full-custom process. With  $T$ ,  $B_F$ ,  $f_1$ ,  $f_2$ , and  $f_{c,\min}$  assumed to be 300 K, 100, 100 Hz, 10 kHz, and 100 Hz, respectively, (15)–(18) result in

$$\begin{aligned} I_1 &= 1.6 \mu\text{A}, & I_2 &= 120 \text{ nA}, \\ R_1 &= 16 \text{ k}\Omega, & R_2 &= 220 \text{ k}\Omega \end{aligned}$$

For  $R_f$  a 6-k $\Omega$  resistor has been chosen.  $I_f$  therefore varies between 1.5 and 11  $\mu\text{A}$ .

## 7. Measurements

The communication between the filter and the measuring instruments was done as follows. In order to perform the voltage-current conversion, a 100-M $\Omega$  resistor has been chosen. The output signal was made measurable by an op amp with a 1-M $\Omega$  resistor in transimpedance configuration, to perform the current-voltage conversion. For three different values of the control current  $I_f$ , corresponding with cutoff frequencies of 100, 320, and 1000 Hz, respectively, the gain and phase of the transfer were measured. The result is shown in figure 7. We observe a second-order Butterworth characteristic between 10 Hz and 10 kHz. The loss in the passband is less than 1 dB. The bandwidth equals 10 kHz. The filter linearity has been evaluated measuring the total harmonic distortion for various input signals. The maximum current (at both the input and output) corresponding to a 5% total harmonic distortion amounts to 25 nA (peakvalue). Combining this number with the measured output noise of 57 pA<sub>rms</sub>

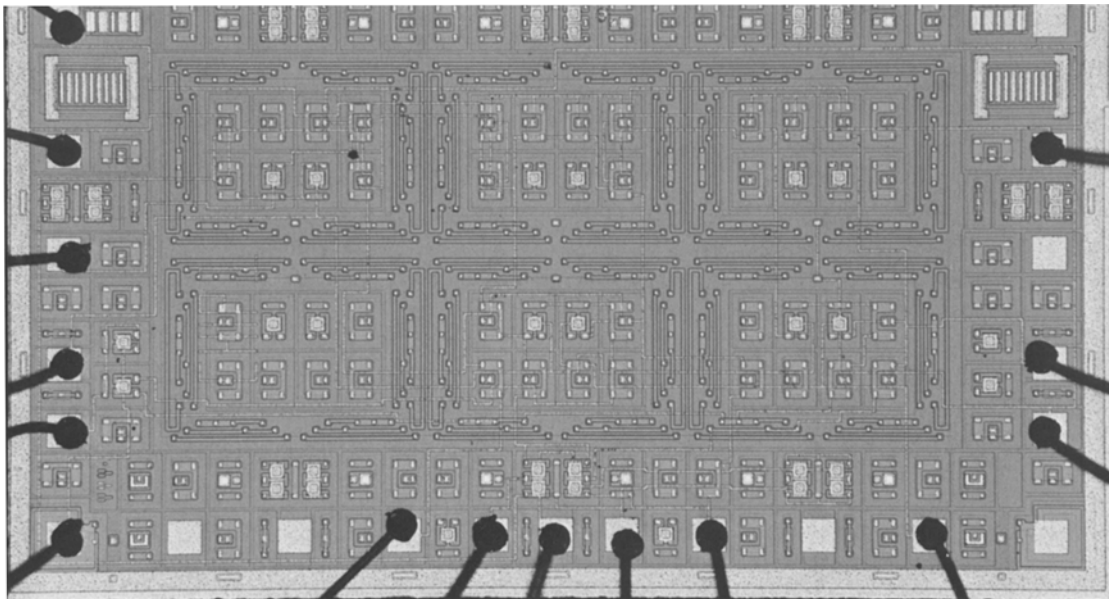


Fig. 6 Microphotograph of the semicustom chip.

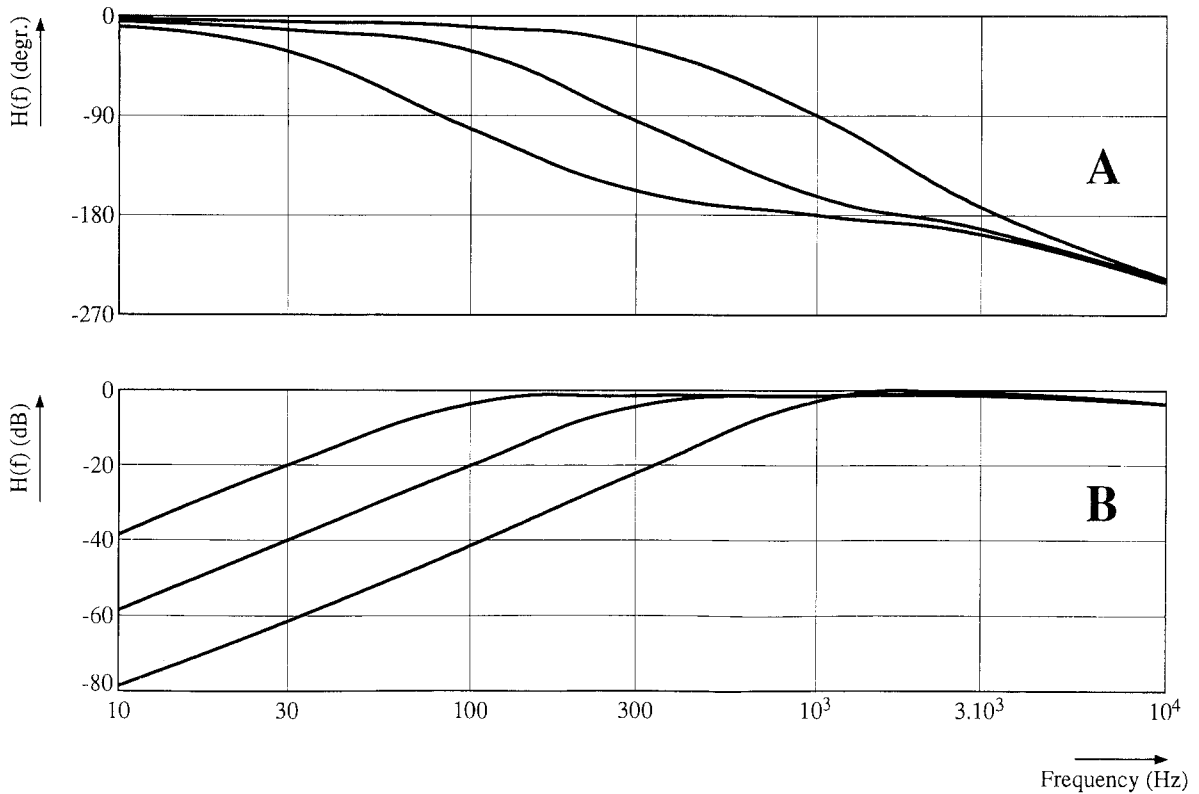


Fig. 7. Phase (A) and gain (B) transfer of the filter.

results in a dynamic range of 50 dB. The filter operates well at voltages down to 1.0 V and consumes less than 16  $\mu$ A. No instability occurs.

**8. Conclusions**

A low-power, low-voltage fully integrated second-order high-pass filter has been presented that works in the current domain. The filter is a two-integrator type, in which an integrator is realized by a capacitance and an adjustable transconductance amplifier with an indirect output. The test chip demonstrates operation down to 1 V with less than 16  $\mu$ W power consumption and a dynamic range of 50 dB.

**9. Appendix: Noise Transformation**

In order to find an expression for the equivalent noise current at the output of the integrator we will use the simple noise model of the bipolar transistor as presented in figure 8 [16].

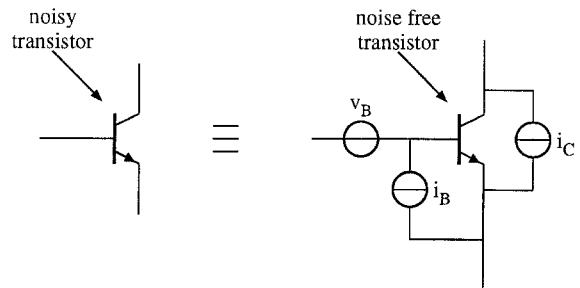


Fig. 8. Representation of a noisy transistor by a noise free transistor together with two noise current sources and one noise voltage source.

In the bipolar transistor two noise sources are found whose spectra are proportional to the bias current: the shot noise ( $i_C$ ) of the collector current, with a power density spectrum (in  $A^2/Hz$ )  $S(i_C) = 2qI_C$ , and the shot noise ( $i_B$ ) of the base current, with spectrum  $S(i_B) = 2qI_B$ . Bipolar transistors also produce thermal noise due to their base resistance  $R_B$ . Its power density spectrum  $S(v_B)$  (in  $V^2/Hz$ ) equals  $4kTR_B$ .

By using  $g_m = qI_C/kT$  and  $I_B = I_C/B_F$  we are able to transform  $i_C$  to the input into two (correlated) noise sources  $v_n = i_C/g_m$  and  $i_n \approx i_C/B_F$  (low-frequency

approximation). See figure 9. As  $S(v_B) = 4kTR_B$  and  $S(v_n) (=S(i_C)/g_m^2 = 2qI_C/g_m^2)$  equals  $4kT/2g_m$ ,  $v_B$  is negligible if  $R_B \ll 1/2 g_m$ . A typical value of  $R_B$  is 500  $\Omega$ . Therefore the influence of  $R_B$  can be neglected as long as  $I_C$  does not exceed several tens of microamps. As  $S(i_B) = 2qI_B$  and  $S(i_n) (\approx S(i_C)/B_F^2 = 2qI_C/B_F^2)$  approximately equals  $2qI_B/B_F$ ,  $i_n$  is always negligible with respect to  $i_B$ . The remaining two (uncorrelated) sources  $v_n$  and  $i_B$  can be summed in one voltage source  $v_{in}$  in series with the capacitor using the Blakesley transformation for voltage sources and an equivalent transformation for current sources (see [12], for example). We find

$$\begin{aligned} S(v_{in}) &= S(v_n) + S(i_B) \left( R^2 + \frac{1}{4\pi^2 f^2 C^2} \right) \\ &= \frac{2kT}{g_m} + \frac{2kTg_m}{B_F} \left( R^2 + \frac{1}{4\pi^2 f^2 C^2} \right) \end{aligned} \quad (20)$$

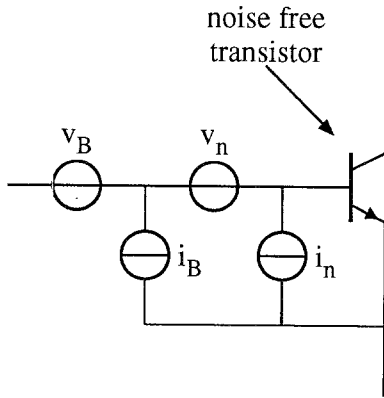


Fig. 9. Representation of the same noisy transistor by a noise-free transistor and four noise sources at the input.

In many practical situations  $1/4\pi^2 f^2 C^2 \gg R^2$ . Therefore  $S(v_{in})$  can be approximated by

$$\begin{aligned} S(v_{in}) &= S(v_n) + S(i_B) \frac{1}{4\pi^2 f^2 C^2} \\ &= \frac{2kT}{g_m} + \frac{2kTg_m}{B_F} \frac{1}{4\pi^2 f^2 C^2} \end{aligned} \quad (21)$$

When  $v_{in}$  is transformed to the output into an equivalent current source  $i_{n,eq}$  we obtain

$$\begin{aligned} S(i_{n,eq}) &= S(v_{in})H_t^2 = S(v_{in}) \frac{1}{n^2 R^2} \\ &= \frac{2kT}{n^2} \left( \frac{1}{R^2 g_m} + \frac{g_m}{4\pi^2 f^2 B_F R^2 C^2} \right) \end{aligned} \quad (22)$$

To obtain  $i_{n,eq}$  we integrate  $S(i_{n,eq})$  over the total audio frequency range (from  $f_1$  to  $f_2$ ) and square-root the result. This results in

$$i_{n,eq} = \sqrt{\frac{2kT(f_2 - f_1)}{n^2} \left( \frac{1}{R^2 g_m} + \frac{g_m}{4\pi^2 B_F f_1 f_2 R^2 C^2} \right)} \quad (23)$$

## Acknowledgment

The author wishes to thank Albert van der Woerd and Rob van Beijnhem for valuable discussions and the Delft Institute for Microelectronics and Submicron Technology (DIMES) for processing the chip.

## References

1. D.W.H. Calder, "Audio frequency gyrator filters for an integrated radio paging receiver," *Proc. IEE Conf. Mobile Radio Syst. Tech.*, pp. 21–24, 1984.
2. I.E. Getreu and I.M. McGregor, "An integrated class-B hearing-aid amplifier," *IEEE J. Solid-State Circuits*, Vol. SC-6, pp. 376–384, 1971.
3. F. Callias, F.H. Salchli, and D. Girard, "A set of four ICs in CMOS technology for a programmable hearing aid," *IEEE J. Solid-State Circuits*, Vol. SC-24, pp. 301–312, 1989.
4. A.C. van der Woerd "Low-voltage low-power infra-red receiver for hearing aids," *Electron. Lett.*, Vol. 28, No. 4, pp. 396–398, 1992.
5. E. Villchur, "Signal processing to improve speech intelligibility in perceptive deafness," *J. Acoust. Soc. Am.*, Vol. 53, pp. 1646–1657, 1973.
6. G. Keller and L. Plath, *Technische Hilfe bei der Rehabilitation Hörgeschädigter*, Springer-Verlag: Berlin, Chap. 1980.
7. A.C. van der Woerd, *Analog Circuit for a Single-Chip Infra-Red Controlled Hearing Aid*, Delft University of Technology, Delft, The Netherlands, to appear.
8. M.E. van Valkenburg, *Analog Filter Design*, Holt, Rinehart and Winston: New York, 1982.
9. M.S. Ghousi and K.R. Laker, *Modern Filter Design*, Prentice-Hall: Englewood Cliffs, NJ, 1981.
10. G. Groenewold, *Optimal Dynamic Range Intergrated Continuous-Time Filters*, Ph.D. Thesis, Delft University of Technology, Delft, The Netherlands, 1992.
11. C. Toumazou, F.J. Lidgley, and D.G. Haigh (ed.), *Analogue IC Design: The Current-Mode Approach*, Peter Peregrinus: London, Chap. 2, 1990.
12. E.H. Nordholt, *Design of High-Performance Negative Feedback Amplifiers*, Elsevier: Amsterdam, 1983.
13. C. Toumazou, F.J. Lidgley, and D.G. Haigh (ed.), *Analogue IC Design: The Current-Mode Approach*, Peter Peregrinus: London, Chap. 6, 1990.
14. R.J. Wiegink, E. Seevinck, and W. de Jager, "Offset cancelling circuit," *IEEE J. Solid-State Circuits*, Vol. SC-24, No. 3, pp. 651–658, 1989.

15. Linear Technology Inc., *Series LA200/LA250 Semicustom Array Design Manual*.
16. P.T.M. van Zeijl, *Fundamental Aspects and Design of an FM Upconversion Receiver Front-End with On-Chip SAW Filters*, Ph.D. thesis, Delft University of Technology, Delft, Chap. 5, 1990.



**Wouter A. Serdijn** was born in Zoetermeer, The Netherlands, in 1966. He received his M.Sc. degree in electrical engineering from the Delft University of Technology, The Netherlands, in 1989. Subsequently he joined the Electronics Laboratory at Delft to work toward a Ph.D. thesis. His research includes developing a formal design theory for low-voltage low-power analog integrated circuits along with the development of circuits for hearing instruments.